THE AMERICAN SOCIETY OF MECHANICAL ENGINEERS
345 E. 47th St., New York, N.Y. 10017

97-GT-193

Turbulent Computations of Internal Flows using an Anisotropic Diffusivity Model

E. LAROCHE

ONERA- Direction de l'Energetique
29, Avenue de la Division Leclerc
BP 72 - 92322 Chatillon
FRANCE

Abstract

The Reynolds analogy is known to give inadequate results for strongly anisotropic turbulence. The use of an anisotropic diffusivity, through the Generalized Gradient Diffusion Hypothesis (GGDH), can partially overcome these deficiencies.

The quality of the heat transfer prediction then relies on the accuracy of the Reynolds stresses estimation, which requires a second order closure. The article presents applications of an Algebraic Stress Model (ASM) coupled with a GGDH to the computations of various internal flows. The computations were done using the NS3D MATHILDA code, developed at ONERA, and largely used in the French aerospace industry.

The study compares the ASM+GGDH results with experimental measurements for heated configurations such as a pipe, a rotor/stator cavity and a channel with ribs, ie covering a wide spectrum of turbine gas internal flows.

The ASM+GGDH model leads to major improvements for the latter case, where the wall fluxes were largely underestimated in a standard k-ε calculation. The difference is due to an overestimation of the turbulent Prandtl number, closer to 0.5 for a mixing layer. The ASM+GGDH model also gives a correct hierarchy of the turbulent heat fluxes for pipe flows, contrary to a standard isotropic model. Concerning the rotor/stator cavity the results are in good agreement with the measurements provided by Owen et al [1].

Nomenclature

C_w	nondimensional flowrate (=m/μb)
D_h	hydraulic diameter
e	rib height
G	gap ratio (=s/R)
k	turbulent kinetic energy, thermal conductivity
m	mass flow rate
Nu	Nusselt number
p	distance between two ribs
Pr	Prandtl number (=$\mu C_p/k$)
Pr_t	turbulent Prandtl number
q_w	convective heat flux
r	radius of disc
R	outer radius
Re_{Dh}	reynolds based on the hydraulic diameter
Re_ω	rotational Reynolds number (=$\Omega R^2/\nu$)
s	axial gap between disks
U_τ	friction velocity
y	distance from the wall
y^+	dimensionless distance from the wall (= pyU_τ/μ)
ε	turbulent energy dissipation rate
χ,χ_t	thermal, turbulent diffusivity
μ,μ_t	dynamic, turbulent viscosity
ρ	density
θ	temperature
Ω	angular velocity of disc

Introduction

A few years ago, the most popular and economical approach to compute heat transfer for internal flows was the use of "wall functions". This approach is based on a Couette type approximation in the near wall region, along with the assumption that turbulence is not far from an equilibrium state, which one encounters, for instance, in the log region of a boundary layer.

Presented at the International Gas Turbine & Aeroengine Congress & Exhibition
Orlando, Florida — June 2-June 5, 1997

Unfortunately, in turbomachinery applications, one mainly deals with complex turbulent flows, where these hypothesis are oversimplified representations of reality. That is why many industrial computations are now based on Low-Reynolds two equation models. These models allow a better description of the near-wall region, which is fundamental for the estimation of the heat transfer.

However, they do not account for strong anisotropy effects, and the heat fluxes are mostly evaluated through the Reynolds analogy. The thermal turbulent diffusivity is derived from the eddy viscosity, and the turbulent Prandtl number is assumed to be constant .

There is a commonly accepted value of this number (Prt=0.9), based on the mean value of the heat transfer inside a boundary layer. However, the use of a uniform Prt has given disappointing results in many complex situations, even when the aerodynamic field was correctly predicted.

To take into account the anisotropic thermal effects, the best approach would be to compute the full system of transport equations, using a second order modeling for both aerodynamic and thermal quantities.

However, for industrial applications, this is still an unrealistic challenge and we decided to adopt a simplified approach, using an explicit Algebraic Stress Model (ASM) to compute the Reynolds stresses [2][3][4], and an extension of the Generalized Gradient Diffusion Hypothesis for the thermal fluctuations.

This paper presents several applications of this higher-order treatment of heat transfer equations, using the MATHILDA code developed at ONERA.

Numerical methods

The MATHILDA code solves the unsteady tridimensionnal Navier-Stokes equations, averaged in the Reynolds meaning, for a mixture of perfect gases [5].The discretization is based on finite volume techniques on curvilinear structured grids.

The time integration is either explicit, then a predictor-corrector scheme is used, or implicit with first or second-order accuracy. The implicit algorithm uses a classical ADI factorisation. All the calculations presented below were carried out using the implicit algorithm, with second-order accuracy, to obtain the stationary solution.

The spatial discretization scheme is second-order accurate. The Euler fluxes are evaluated through a "Flux Difference Splitting" TVD scheme. The viscous fluxes are calculated at the center of cells and then interpolated on the cell interfaces.

Turbulence modeling

Reynolds Stress Modeling

MATHILDA standard model is a two equation k-l model, based on Boussinesq approximation, which assumes that turbulent stresses are proportional to the gradients of the mean flow :

$$\overline{u_i u_j} = \frac{2}{3} K \delta_{ij} - \nu_t \left(\frac{\partial U_i}{\partial x_j} + \frac{\partial U_j}{\partial x_i}\right), \quad (1)$$

The eddy viscosity is then related to the turbulent scales through the closure relation :

$$\nu_t = C_\nu f_\nu \sqrt{k} L \qquad (2)$$

where k and L are respectively the turbulent kinetic energy and the mixing length, and Cv=0.548. The transport equations for k and l read:

$$\frac{Dk}{Dt} = P - \varepsilon + \nabla.\left((\nu + \frac{\nu_t}{\sigma_k})\nabla k\right)$$

$$\frac{DL}{Dt} = \frac{\nu\alpha}{L}(\chi^2 - \nabla L \nabla L) + \frac{\nu_t}{\sigma_l L}(\psi\chi^2 - \nabla L \nabla L) \qquad (3)$$

$$- \nabla L.(1 + 0.5 * (1 - f_\nu^2) R_T / (A_\nu f_\nu)(0.5 \frac{L}{K} \nabla K + \nabla L))$$

where,

$$\varepsilon = f_\varepsilon C_\varepsilon \frac{k^{3/2}}{L} + 2\chi^2 \nu \frac{k}{L^2}, \quad \psi = 1 + 0.125 * (\frac{P}{\varepsilon} - 1), \quad P = 2\nu_t S^2$$

$$\sigma_k = 1.0, \quad \sigma_L = 1.3, \quad \alpha = 0.4, \quad C_\varepsilon = 0.164$$

$$f_\nu = \tanh(\frac{R_T}{2A_\nu}), \quad f_\varepsilon = \tanh(\frac{R_T}{2A_\varepsilon}), \quad R_T = \frac{\nu_t}{\nu}$$

$$A_\nu = 10.65, \quad A_\varepsilon = 8.00$$

This k-l model is nearly equivalent to a standard k-ε model, except near the walls, where it is much more robust from a numerical point of view. The model also includes low-Reynolds number corrections, such as the term f_ν of (2), to account for the damping effect of molecular viscosity near the wall. A RNG extension of the standard k-l model generally improves the results of this two-equation model, at least for 2D flows with strong recirculations or high curvatures [6][7][8][9][10].

These eddy viscosity models (EVM) are not adapted to the computation of strongly anisotropic flows, where a second-order closure is required. The use of the explicit Algebraic Stress Model (ASM) of MATHILDA is recommended for such flows. This model is derived from the exact transport equation for Reynolds stresses which accounts for anisotropy. The ASM model expresses transport of $\overline{u_i u_j}$ in terms of that of k, neglecting the variation of the anisotropy tensor along a stream line :

$$\frac{D\overline{u_i u_j}}{Dt} = \frac{\overline{u_i u_j}}{k} \frac{Dk}{Dt} \qquad (4)$$

Originally valid for homogeneous flows and fully developed turbulence, the model was extended to near-wall flows, through the addition of low-Reynolds number corrections. This model provides a correct estimation of the Reynolds stress tensor and results in major improvements in the prediction of rotating and secondary flows.

Heat Transport Modeling

MATHILDA usually computes turbulent heat fluxes through an isotropic turbulent diffusivity χ_t.

$$-\overline{u_i\theta} = \chi_t \frac{\partial \Theta}{\partial x_i} \qquad (5)$$

According to the Reynolds analogy, this diffusivity is proportional to the eddy viscosity through the turbulent Prandtl number Pr_t [11][12][13]:

$$\chi_t = \frac{\nu_t}{Pr_t} \qquad (6)$$

For flows with strong thermal anisotropies, an extended version of the Generalized Gradient Diffusion Hypothesis, coupled to an ASM calculation was used [14][15][16]. It is similarly derived from the transport equations for $\overline{u_i\theta}$, which reads (in the high Reynolds number limit) :

$$\frac{D\overline{u_i\theta}}{Dt} = -\left\{\overline{u_iu_k}\frac{\partial\theta}{\partial x_k} + \overline{\theta u_k}\frac{\partial U_i}{\partial x_k}\right\} + \overline{f_i\theta} + \phi_{i\theta} - \varepsilon_{i\theta} - d_{i\theta} \qquad (7)$$

where,

$$\phi_{i\theta} = \overline{\frac{p}{\rho}\frac{\partial\theta}{\partial x_i}}$$

$$\varepsilon_{i\theta} = \nu\left[\overline{\frac{\partial\theta}{\partial x_k}\left(\frac{\partial u_i}{\partial x_k} + \frac{\partial u_k}{\partial x_i}\right)} + \frac{1}{\sigma}\overline{\frac{\partial u_i}{\partial x_k}\frac{\partial\theta}{\partial x_k}}\right]$$

$$d_{i\theta} = \frac{\partial}{\partial x_k}\left[\overline{u_i\theta u_k} + \overline{\frac{p\theta}{\rho}}\delta_{ik} - \nu\left(\overline{\theta\frac{\partial u_i}{\partial x_k}} + \overline{\theta\frac{\partial u_k}{\partial x_i}} + \frac{1}{\sigma}\overline{u_i\frac{\partial\theta}{\partial x_k}}\right)\right] \qquad (8)$$

$\phi_{i\theta}$ is modelled as follows :

$$\phi_{i\theta} = -c_1\frac{\varepsilon}{k}\overline{u_i\theta} + c_2\overline{\theta u_k}\frac{\partial U_i}{\partial x_k} \qquad (9)$$

(neglecting the wall-reflection parts of the pressure interaction)

Here the convective derivative is approximated using the hypothesis of local equilibrium for $\frac{\overline{u_i\theta}}{\sqrt{k\overline{\theta^2}}}$

$$\frac{D\overline{u_i\theta}}{Dt} = \frac{0.5\overline{u_i\theta}}{\sqrt{k\overline{\theta^2}}}(P - \varepsilon + P_{i\theta} - \varepsilon_{i\theta}) \qquad (10)$$

A further simplification is made, assuming $\overline{\theta^2}$ in local equilibrium $P_{i\theta} = \varepsilon_{i\theta}$. Neglecting the turbulent tranport $d_{i\theta}$ and $\varepsilon_{i\theta}$, (7) now reads :

$$-\langle u_i\theta\rangle / k = \frac{\langle u_iu_m\rangle\frac{\partial\Theta}{\partial x_m} + (1-C_2)\left(\langle u_m\theta\rangle\frac{\partial U_i}{\partial x_m}\right)}{\varepsilon\left[C_1 + 0.5\left(\frac{P_k}{\varepsilon} - 1\right)\right]}$$

$$P_k = -\langle u_mu_n\rangle\frac{\partial U_m}{\partial x_n} \qquad (11)$$

where,

C_1=3.2, C_2=0.5

The second RHS term makes the system an implicit one. To get a first idea of the effects of an anisotropic thermal model, this term was first neglected. Therefore, the model implemented in MATHILDA is a generalization of the classical GGDH hypothesis :

$$-\langle u_i\theta\rangle / k = \frac{\langle u_iu_m\rangle\frac{\partial\Theta}{\partial x_m}}{\varepsilon\left[C_{T1} + 0.5\left(\frac{P_k}{\varepsilon} - 1\right)\right]} \qquad (12)$$

The next step in the model will consist in taking into account this term. The validity of this model strongly depends on an accurate evaluation of the Reynolds stresses, and is therefore meant to be coupled with the use of an ASM or RSM extension. The validations presented below compare the behavior of this ASM + GGDH model, with results obtained through a classical approach. This model was derived using a High-Reynolds formulation. Therefore all the calculations were performed using wall functions. The modification of the heat transfer coefficient mainly comes from the improvements of the temperature field prediction as the turbulent contribution to the heat fluxes decreases near the wall.

An equivalent directional turbulent Prandtl number can be estimated using a simplified version of (11). Taking into account only the normal to the wall component (y for instance) of the temperature gradient, (11) now reads :

$$-\langle u_2\theta\rangle / k = \frac{\langle u_2^2\rangle\frac{\partial\Theta}{\partial y}}{\varepsilon\left[C_{T1} + 0.5\left(\frac{P_k}{\varepsilon} - 1\right)\right]} \qquad (13)$$

In other terms, for each computation point

$$Pr_{teq2} = \frac{C_\mu k}{\langle u_2^2 \rangle}\left[C_{T1} + 0.5\left(\frac{P_k}{\varepsilon} - 1\right)\right] \quad (14)$$

A Low-Reynolds number correction is still under study and is of critical interest, since the anisotropies are particularly strong near the wall.

Validation-Industrial applications

The model was tested on various configurations. The computations on academic tests first made sure that the model behaved properly for well-known configurations.

The first geometry was a heated pipe flow, where the Nusselt number is given by the Dittus Boelter correlation :

$$Nu = 0.023\ Re^{0.8}\ Pr^{0.4}$$

The Reynolds number of the air (Pr=0.72) bulk flow is 406000 and a uniform heat flux of 300 W/m^2 is enforced on the wall. The ASM + GGDH leads to Nu=620, which is fairly close to the D-B correlation (Nu=618).

Our main concern was to evaluate the possible benefits of this model for the computation of internal flows. The focus was put on two configurations typical of the cooling systems encountered in turbomachinery.

a/ Rotor/stator cavity

The first test case is an air cooled rotor/stator system, which was studied by OWEN (1994) et. al (Re=1.25E6,Cw=6100,G=0.12). The rig consisted of an electrically-heated rotating disk (rotor) close to an unheated stationary disk (stator). A radial outflow was used to cool the rotor and fluxmeters measured the local Nusselt numbers at different radius locations. The experimental data were compared to computations carried out with a Low-Reynolds k-ε, on a very fine grid, with a satisfactory agreement [1].

Grid distribution

Computations were carried out on a relatively coarse mesh (95*60), with a contraction parameter around 1.1 (Fig 1). For the first point, y^+=30, at the edge of the log region. There was no significative difference between the results obtained with that grid (using wall laws) and a finer one where y^+=1 for the first point (using a Low Reynolds number correction). This is due to the k-l model of MATHILDA, where the usual cross diffusion term (depending on the gradient of k) is ignored. The velocity profiles were very similar, the difference for the Nusselt number was within a 10 % range. It confirms that the wall laws provide an appropriate treatment of the near-wall region. Performing a calculation on a coarse grid to be able to use the ASM+GGDH model was therefore reasonable.

Boundary conditions

At the inlet the mass rate and temperature were specified. Part of the upstream pipe was taken into account to get a proper description of the entrance effects.

The stator and shrouds were specified as adiabatic, whereas the the measured temperature profile was used as the thermal boundary condition on the rotor.At the outlet, the pressure was specified as atmospheric

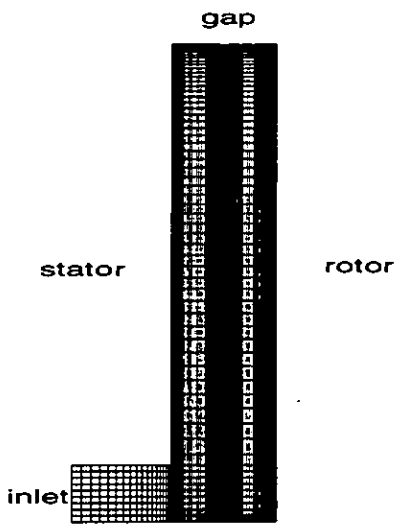

Fig. 1 : rotor-stator system, computational grid

Comparison between computations and experiments

Fig. 2 shows a comparison between the computed and measured non-dimensional radial and circumferential velocities. The good agreement obtained here was a preliminary condition to any ASM+GGDH computation. Had the results been far from the experimental data, there would not have been any interest in examining the Nusselt number profile. Even these satisfying results for the radial and circumferential velocities are in no way a reliable indication that the computed Reynolds stresses are valid, the gradients being negligible in the core region. Fig. 3 shows the comparisons between the computed and measured local Nusselt numbers on the rotor.

The local Nusselt number is defined as :

$$Nu = \frac{q_o r}{k(\theta_o - \theta_{ref})}$$

θ_{ref} is taken as the inlet temperature. The ASM+GGDH model is also compared to the results obtained with a classical k-l model where Pr_t=0.9. The agreement is satisfying (10 % in the upper part of the cavity). A Low Reynolds model would probably correct this underestimation, through a better description of the Ekman layer. Some of the constants of the GGDH model are still adjustable.

The evaluation of an equivalent Prt in the core region gives Prt=0.8-0.9, which is close to the standard value. This result explains the relatively good agreement between the classical and GGDH approaches.

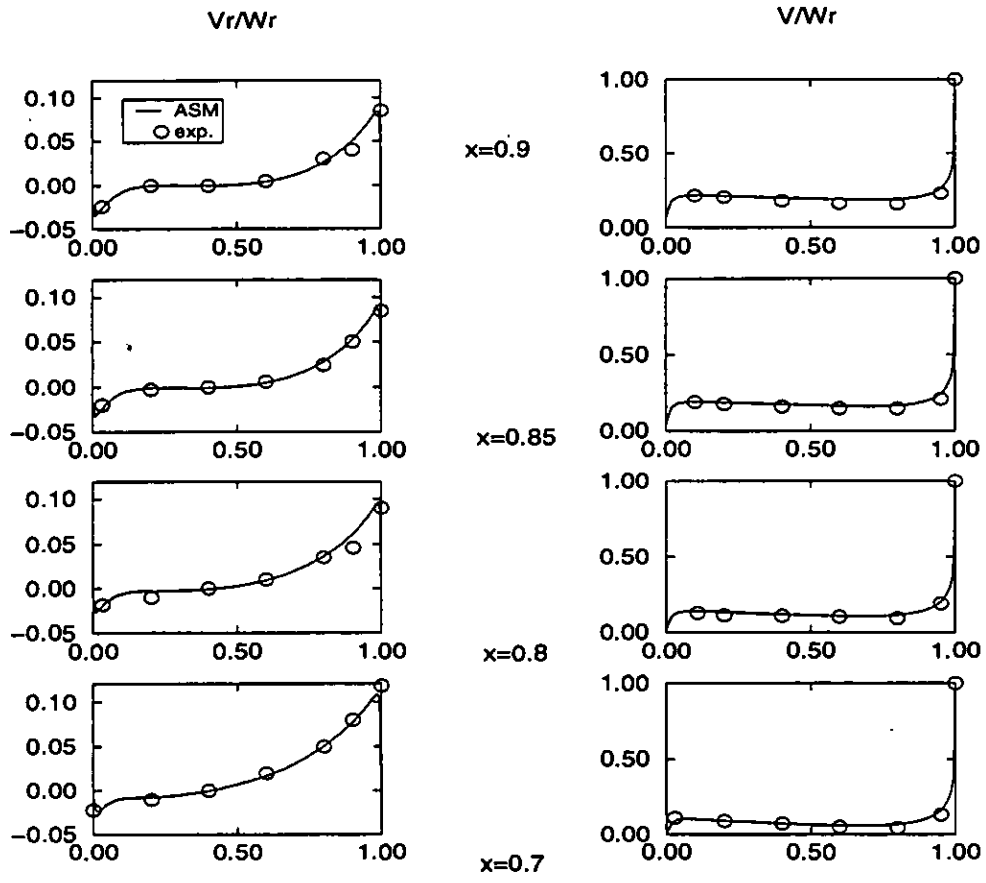

Fig. 2 : Computed and measured velocity profiles for the rotor-stator system

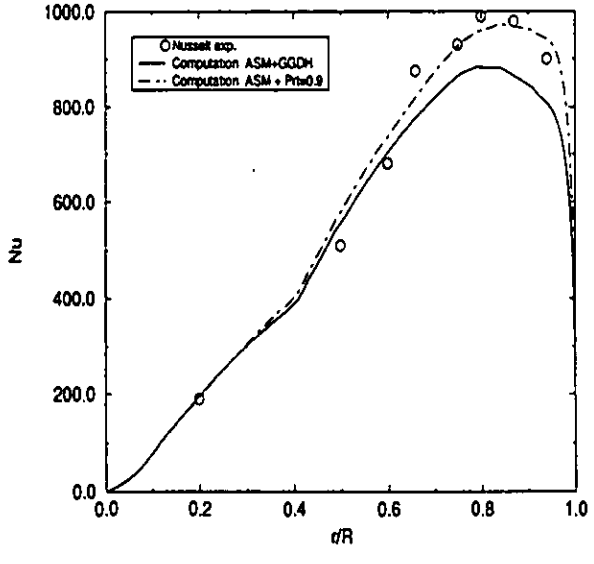

Fig. 3 : Computed and measured Nusselt profiles along the rotor

b/ rib roughened channel

The second representative configuration is that of a rib roughened channel, studied at the Von Karman Institute [17]. Rib roughened surfaces are a very efficient and widespread means of cooling internally high pressure turbine components. These components operate at very high temperatures, largely above the melting point. Rib roughened channels enhance the heat transfer but they create complex recirculating flows, whose prediction is still difficult.

Experiments were conducted on straight rectangular channels with various rib arrangements, in order to optimize the heat transfer efficiency. One of the configurations was selected as a benchmarch test for the ASM+GGDH model. So far, the classical approach has failed to correctly predict the measured heat transfer [18]. All the isotropic diffusivity models lead to an underestimation of the heat fluxes. The difference can be of 40 to 50 %, even when the aerodynamic results are satisfying.

The channel has the following characteristics :

- only one wall is ribbed, with ribs normal to the flow direction
- e=10 mm, Dh=10 cm, ie 10% blockage
- pitch to height ratio (p/e) = 9
- Reynolds number of the bulk flow (Rdh=30000)

Grid distribution - Boundary conditions

2D Computations were conducted on a relatively coarse grid (438*45), with 10 cells on the rib height (Fig. 4). The first grid point is located at y^+=20. A computation was performed on a finer mesh (439*65), with the first grid point at y^+=1 (using a Low-Reynolds number correction). There was no significant difference in the aerodynamic field and the computations were therefore carried out on the coarse grid for the anisotropic thermal model. Wall functions provide an appropriate treatment of the near-wall region.The mass rate is specified at the inlet, the atmospheric pressure is applied at the outlet, and a uniform heat flux provides the thermal boundary condition.

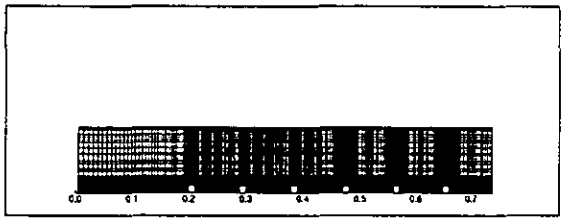

Fig. 4 : Rib roughened channel, computational grid

Comparison between computations and experiments

Aerodynamic results

The presence of the rib reduces the cross-section of the channel, therefore causing the acceleration of the flow in front of each rib. The sudden expansion after a rib creates a separation zone. The flow reattaches after x/e=4-5 and a new boundary layer is formed. The flow becomes periodic after 3 ribs for both experimental and computational data and all the following analysis will be carried out on that part of the system (Fig 5)

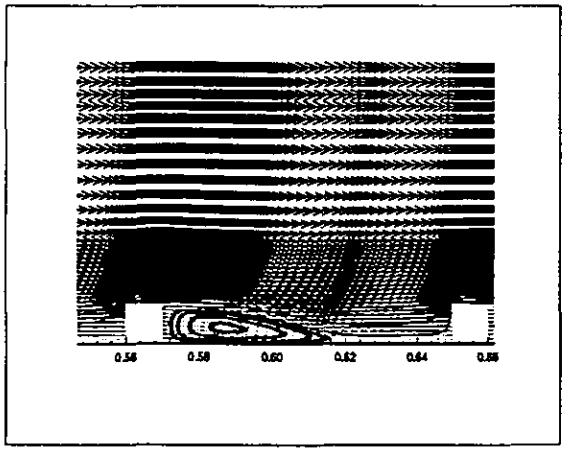

Fig 5 : Velocity streamlines

Experimentally, this configuration was found to be the limit between the existence and the absence of a reattachment point.

There is a good agreement between measured and calculated contours except in the near-wall region. The estimated recirculation length is about 5 times the rib height, while the measurements indicate a value of 4.3 times the rib height. The estimation of k is also close to the experimental values (the main problem coming from the l-equation).

These aerodynamic results were globally found satisfactory (Fig 6). They were close to those provided by a standard k-l model and any major difference on the thermal results is mainly due to the thermal model itself.

3D computations with a classical k-l model were also carried out and gave a reattachment point with a correct recirculation lenght, but the heat transfer coefficient maximum in the symmetry plane was unchanged.

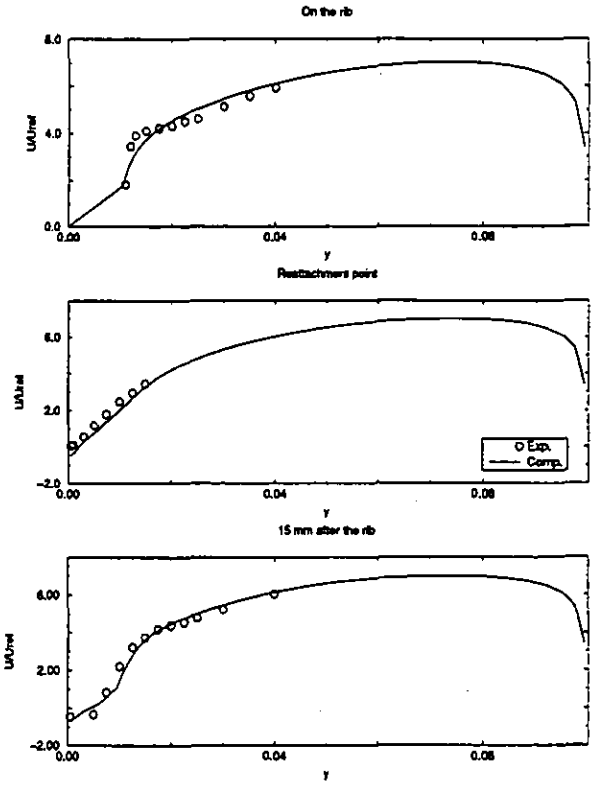

Fig. 6: Computed and measured velocity profiles

Thermal results

The local Nusselt number is defined as :

$$Nu = \frac{q_o D_h}{k(T_o - T_{ref})}$$

where k is the thermal conductivity. T_{ref} was taken to be the inlet temperature. Rigourously, T_{ref} should be the average bulk temperature, but the temperature variation between the inlet and the outlet is negligible.

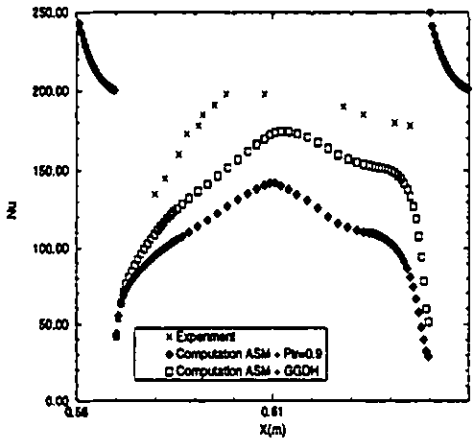

Fig 7 : Computed and measured profiles between the ribs.

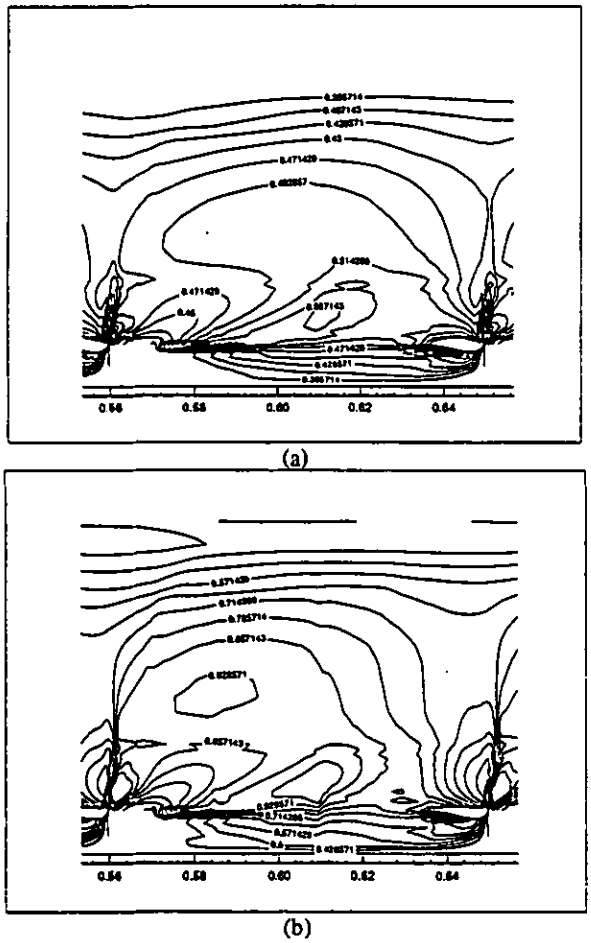

(a)

(b)

Fig. 8 : Equivalent Turbulent Prandtl number in the X direction (a) , Y direction (b)

Local Nusselt number distributions are presented on Fig.7. The comparison between experimental and computational results is poor for classical approaches.The estimation of the location of the maximum of the Nusselt number with an ASM+GGDH model is still poor.

But, this comes from the aerodynamical prediction, as there is a strong correlation between the reattachment point and the maximum of the heat transfer. Therefore, as the ASM overestimates the recirculation length, the prediction of the position of the heat transfer maximum is also wrong. What is more interesting is that the standard thermal model underestimates heat transfer by 30 to 50 %, the most important discrepancy being upstream the rib.The ASM + GGDH considerably improves the Nusselt number prediction. The difference between computational and measured values now ranges from 10 to 25 %.

An equivalent directional turbulent Prandtl number can also be evaluated using the velocity-temperature correlations and the Reynolds-stresses. Fig.8 shows the contours of Prt in the X and Y directions. It varies from 0.3 to 1.1 in the direction normal to the wall (Y), and from 0.35 to 0.55 for the mean flow direction (X). The ratio of these directional Prandtl numbers quantifies the anisotropy of the flow. Due to the strong anisotropies of the velocity and temperature fields, they are far from the standard 0.9 value and this explains the poor results obtained until now, assuming Pr_t constant.These estimations of the turbulent Prandtl are in rather poor agreement with measurements by Fujita and al [19], who suggested a value of about 0.5 between the ribs and of 0.7 in the upper part of the channel (Fig. 9). However, they give a better approximation of the equivalent Prandtl number, especially near the wall, and for the upper part of the channel. The measurements by Fujita and al were obtained comparing the slopes of the logarithmic laws for the velocity and the temperature fields, near a side wall and therefore, are not strictly valid in the mid plane. However, they confirm that the concept of a uniform Prandtl number everywhere in a cross-section is not valid for a rough duct and they show the decrease of the Prandtl number near the rough wall, which corresponds to an increase in the heat transfer , as the wall fluxes are very dependent on the near-wall flow.

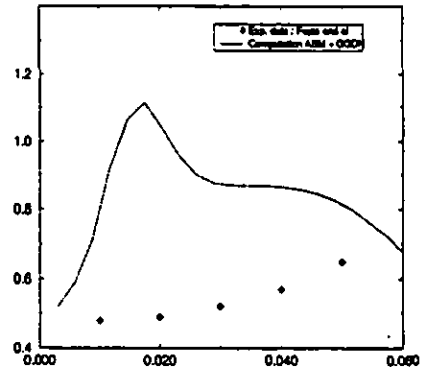

Fig 9 : Distributions of turbulent Prandtl number for X=0.61 m

The results presented here are essentially valid between the ribs. The simplifications made to derive the model (neglecting the dependance of the heat fluxes with the velocity gradients) are not true near the ribs.

However, taking into account the effects of the anisotropies on the heat fluxes is a significative improvement compared with the standard uniformity hypothesis, and a reasonable simplification before evaluating the influence of velocity gradients. Furthermore, this model is really inexpensive in terms of CPU time, as it only requires an algebraic evaluation of the heat fluxes

Conclusion

The work reported in this article clearly shows the limitations of a uniform turbulent Prandtl number hypothesis to compute complex turbulent flows. A second order-closure for the velocity-temperature correlations is more appropriate as a correct thermal estimation not only requires an adapted aerodynamic description but also a valid thermal modelling.

The thermal model introduced above is directly derived from the transport equations for $\overline{u_i\theta}$. The thermal diffusivity is not computed using the eddy viscosity anymore, therefore allowing the description of anisotropic flows. Compared with a classical GGDH hypothesis, it takes into account the production/dissipation ratio. This kind of model should therefore be more adapted for flows not departing much from an equilibrium state.

The model has been tested on various configurations. The agreement between experimental and computational results was generally good, and for strong anisotropic flows such as those encountered in rib roughened channels,the estimation of the heat transfer is greatly improved. Thus, the difference between computed and measured local Nusselt numbers varies between 10 and 20 % instead of an average value of 40% before.

These improvements are still partial. The dependance with the mean velocity gradients is still to be considered. This dependance was already ignored with a classical model but is particularly relevant for strongly sheared flows.

The model has still to be validated for free flows and 3D geometries, to ensure a reasonable agreement on a fairly large number of configurations.

Acknowledgements

The author would like to thank SNECMA (Societe Nationale d'Etude et de Construction de Moteurs d'Aviation) for their funding. Part of this work comes from a fruitful cooperation with the YKLR department and I am really glad to aknowledge the contributions of D. Fernandez and J. Vialonga in particular. This paper also owes much to the ideas and appropriate suggestions of D. Dutoya, from ONERA.

References

1.J.X Chen, X. Gan, and M.J. Owen - 1994 - Heat Transfer in air-cooled rotor -stator system - ASME Paper - GT - 55

2. B.E Launder, W.C. Reynolds, W. Rodi, J. Mathieu, D. Jeandel - Turbulence Models and their applications, Eyrolles, Vol 2

3. T.B Gatski , C.G. Speziale - 1993 - On Explicit Algebraic Stress Models for Complex Turbulent Flows, J. Fluid Mechanics, Vol. 254, pp 59-78

4. E. Laroche - 1996- Amélioration des modèles de turbulence de MATHILDA par la prise en compte des effets d'anisotropie : modèles ASM et RSM - RT ONERA 6/3758 EY

5. D. Dutoya, M.P. Errera - 1991 - Le code MATHILDA. Modèles physiques, réseau de calcul et méthode numérique. Rapport thechnique ONERA n°42/3473EN

6. V. Yakhot, S. A. Orszag - 1986 - Renormalization Group Analysis of Turbulence - J. Sci. Comput. 1, 3.

7. L. Smith and W.C. Reynolds - 1992 - On the Yakhot-Orszag Renormalization Group for Deriving Turbulence Statistics and Models - Phys. Fluids A, Vol. 4, No. 2

8. V. Yakhot, S. A. Orszag, C.G. Speziale, S. Thangam and T.B. Gatski - 1992 - Development of turbulence models shear flows by a double expansion technique - Phys. Fluids A, Vol 4, No. 7

9. V. Yakhot and L. Smith - 1992- The Renormalization Group, the ϵ-Expansion and Derivation of Turbulence Models, J. Sci. Comput, 7, 1.

10 C.G. Speziale and S. Thangam - 1992 - Analysis of an RNG based Turbulence Model for Separated Flows - Nasa CR-1B9600, ICASE Report NO 92-3

11. J.O Hinze, Turbulence, 2nd edition, McGraw-Hill (1987)

12. S.V. Patankar, D.B. Spalding - 1970 - Heat and Mass Transfer in Boundary Layers, Intertext Books, London

13. J. Cousteix - 1989 - Turbulence et Couche limite, Cepadues

14. T.M. Liou, J.J. Hwang and S.H. Chen - 1993 - Simulation and Measurement of Enhanced Turbulent Heat Transfer in a Channel with Periodic Ribs on One Principal Wall - Int. J. Heat Mass Transfer, Vol 36, No 2, pp507/517

15. C. Benocci - 1991 - Modelling of Turbulent Heat Transport, a State of the Art - VKI Technical Memorandum 47

16. B.E. Launder - 1988- On the Computation of Convective Heat Transfer in Complex Turbulent Flows - J. Heat Transfer, Vol 110, pp 1112-1128

17. G. Rau, M. Cakan, T. Arts - 1996- The effect of Periodic Ribs on the Local Aerodynamic and Heat Tranfer Performance of a straight Cooling Channel - ASME Paper - 96 - GT - 541

18. G. Chaineray - 1995 - Etude théorique et numérique des écoulements et des transferts de chaleur dans les canaux en rotation - Thèse de l'Université Pierre et Marie Curie (Paris VI).

19. H. Fujita, H. Yokosawa and M. Hirota - 1994- Experimental Study on Convective Heat Transfer for Turbulent Flows in a Square Duct with a Ribbed Rough Wall (characteristics of mean temperature field) - Journal of Heat Transfer - Transaction of ASME - Vol. 116 - pp 332-340